Author(s): Knutsen, K. E. & Galeckas, A. & Zubiaga, A. & Tuomisto, Filip & Farlow, G. C. & Svensson, B. G. & Kuznetsov, A. Yu.

Title: Zinc vacancy and oxygen interstitial in ZnO revealed by sequential annealing and electron irradiation

Year: 2012

Version: Final published version

Please cite the original version:

Knutsen, K. E. & Galeckas, A. & Zubiaga, A. & Tuomisto, Filip & Farlow, G. C. & Svensson, B. G. & Kuznetsov, A. Yu. 2012. Zinc vacancy and oxygen interstitial in ZnO revealed by sequential annealing and electron irradiation. Physical Review B. Volume 86, Issue 12. 121203/1-5. ISSN 1098-0121 (printed). DOI: 10.1103/physrevb.86.121203

PHYSICAL REVIEW B **86**, 121203(R) (2012)

Zinc vacancy and oxygen interstitial in ZnO revealed by sequential annealing and electron irradiation

K. E. Knutsen,[1] A. Galeckas,[1] A. Zubiaga,[2] F. Tuomisto,[2] G. C. Farlow,[3] B. G. Svensson,[1] and A. Yu. Kuznetsov[1]

[1]*Department of Physics, Centre for Materials Science and Nanotechnology, University of Oslo, N-0318 Oslo, Norway*

[2]*Department of Applied Physics, Aalto University, P.O. Box 11100, FI-00076 Aalto, Finland*

[3]*Physics Department, Wright State University, Dayton, Ohio 45435, USA*

(Received 26 April 2012; revised manuscript received 22 August 2012; published 24 September 2012)

By combining results from positron annihilation and photoluminescence spectroscopy with data from Hall effect measurements, the characteristic deep level emission centered at ∼1.75 eV and exhibiting an activation energy of thermal quenching of 11.5 meV is associated with the zinc vacancy. Further, a strong indication that oxygen interstitials act as a dominating acceptor is derived from the analysis of charge carrier losses induced by electron irradiation with variable energy below and above the threshold for Zn-atom displacement. We also demonstrate that the commonly observed green emission is related to an extrinsic acceptorlike impurity, which may be readily passivated by oxygen vacancies.

DOI: 10.1103/PhysRevB.86.121203 PACS number(s): 78.55.Et, 61.72.jn, 61.80.Fe, 78.70.Bj

Introduction. Zinc oxide is a wide direct band-gap material of high potential in optoelectronic applications. However, a significant issue holding back the ZnO development is the lack of reliable *p*-type doping.[1] In spite of reports of *p*-type conductivity, the reproducibility is poor. Unintentionally doped ZnO material exhibits *n*-type conduction and typically has a carrier concentration in the range 10^{16}–10^{17} cm^{-3}. Certain controversies exist in the literature regarding the cause of this *n*-type conductivity as well as its intrinsic or extrinsic nature.[2] The key intrinsic point defects to be considered are interstitial zinc (Zn_i), zinc vacancy (V_{Zn}), interstitial oxygen (O_i), and oxygen vacancy (V_O), along with their complexes. Some of these defects, such as V_O and Zn_i, are acting as donors and are believed to be at the root of the *p*-type issue due to a decrease of their formation energy with lowering of the Fermi level position.[3] A reliable spectroscopic identification of intrinsic defects is one of the key prerequisites for resolving these issues. Using photoluminescence, V_{Zn} has been identified previously as being responsible for the emissions centered around 2.35 eV,[4] while V_O has been related to emissions at 2.53 eV (Ref. 4) and 2.42 eV.[5] The latter line has also been attributed to O_{Zn} (2.38 eV)[6] and Cu impurities (2.4 eV).[7] Identification of V_{Zn} luminescence emission at ∼1.6 eV has also been reported using depth-resolved cathodoluminescence spectroscopy combined with positron annihilation spectroscopy (PAS).[8] However, the multitude of uncertain identifications of these emissions adds to the controversy described above, and makes conclusive answers difficult to find in literature.

In the present Rapid Communication, intrinsic point defects in ZnO have been studied by altering their balance by means of variable energy electron irradiation and thermal processing in oxidizing (O_2) and reducing (Zn-vapor) atmosphere. For the sample analysis, PAS and photoluminescence (PL) spectroscopy have been employed in combination with Hall effect measurements. One way of altering the concentration of intrinsic defects is by annealing in different atmospheres to change the chemical equilibrium.[9] Another way, by using variable energy electron irradiation, enables the introduction of point defects selectively on different sublattices.[9–11] Assuming, in a first approximation, equal energy thresholds of atom displacement for zinc and oxygen sublattices [E_d(O) = E_d(Zn)], then in the lower electron energy range one can expect damage solely on the oxygen sublattice with a corresponding increase of O_i and V_O defect concentrations. This is due to the large difference in mass between the electron and the lattice atoms and the fact that the maximum transferred energy (E_{max}) from an electron to a lattice atom is lowered as the atom mass increases. Once the threshold energy is exceeded, i.e., $E_{max} > E_d$, the defect production increases as a function of irradiation energy. As the electron energy is increased further, defect production will gradually start to appear also on the zinc sublattice (V_{Zn} and Zn_i) and may eventually become the dominant contribution. Besides the electron irradiation induced defects, the initial balance of intrinsic defects can also be altered in a controlled fashion by thermal treatment in reducing and oxidizing ambient. More specifically, V_{Zn} and O_i have a lower formation energy in oxidizing atmosphere, whereas the generation of Zn_i and V_O is favored in a reducing atmosphere. As such, this experiment is devised to ensure an explicit spectroscopic identification of intrinsic defects in ZnO.

Experiment. As a starting material, nominally undoped melt grown (MG) ZnO from Cermet, Inc. was used. The wafers were 10 × 10 × 0.5 mm^3 in size with a polished O face and a carrier concentration of ∼1 × 10^{17} cm^{-3}. A set of samples was subjected to thermal annealing at 800 °C for 30 min in reducing and oxidizing ambients, whereupon several control samples were cross annealed, by which we mean subsequent annealing in the complementary ambient. Another set of samples was electron irradiated nominally at 300 K using different energies and fluences as listed in Table I.

Steady-state PL spectra were obtained by employing a 325 nm wavelength of a cw He-Cd laser (10 mW) as an excitation source. The emission was collected by a microscope and directed to a fiberoptic spectrometer (HR4000 and USB4000 Ocean Optics). A complementary long-pass optical filter with a 430 nm cutoff wavelength was employed to increase the dynamic range of the deep level related emission,

TABLE I. Irradiation parameters and room temperature Hall data before and after electron irradiation. E is the electron irradiation energy, Φ is the fluence, J is the average current density, and $\eta = \Delta n/\Phi$ is the average carrier removal rate.

E (MeV)	Φ (cm^{-2})	J ($\mu A/cm^2$)	n (cm^{-3}) Preirrad.	n (cm^{-3}) Postirrad.	η (cm^{-1})
0.45	4×10^{17}	1.74	1.0×10^{17}	8.7×10^{16}	0.033
0.6	5×10^{17}	3.74	1.0×10^{17}	5.3×10^{16}	0.094
0.8	5×10^{17}	3.74	1.2×10^{17}	2.0×10^{16}	0.2
1.2	5×10^{17}	3.74	9.8×10^{16}	1.8×10^{13}	$\geqslant$0.2

and temperature-dependent measurements were carried out in the range 10–300 K using a closed-cycle He refrigerator.

Positron lifetime experiments were performed in vacuum at a pressure of 1–5 $\times$ 10^{-6} Torr and a sample temperature in the range 20–300 K, using a fast-fast spectrometer,[12] with a time resolution of 250 ps, giving an error margin of $<$1 ps in the average positron lifetime. A ^{22}NaCl positron source deposited on Al foil was sandwiched between two pieces of the sample. The lifetime spectra consist of a sum of exponential decay components $n(t) = \sum_i I_i \exp(-t/\tau)$, and were analyzed after subtracting three source components, I_{Al}, I_{NaCl}, and $I_{\mathrm{positronium}}$, having lifetimes of 200, 400, and 1500 ps, respectively. Further details on the method can be found in Refs. 13 and 14.

Results and discussion. The electron irradiated samples exhibited a general decrease in charge carrier concentration, which appeared increasingly prominent at higher irradiation energies, and was accompanied by a decrease in electron mobility as illustrated by the Hall effect data in Fig. 1. This decrease in electron mobility is most likely caused by charged impurity scattering. This indicates that the loss of charge carriers is due to compensation by acceptors introduced during the irradiation. In contrast, the deactivation of donors is not anticipated to decrease the electron mobility. The concentration of zinc vacancies, $[V_{\mathrm{Zn}}]$, can be determined

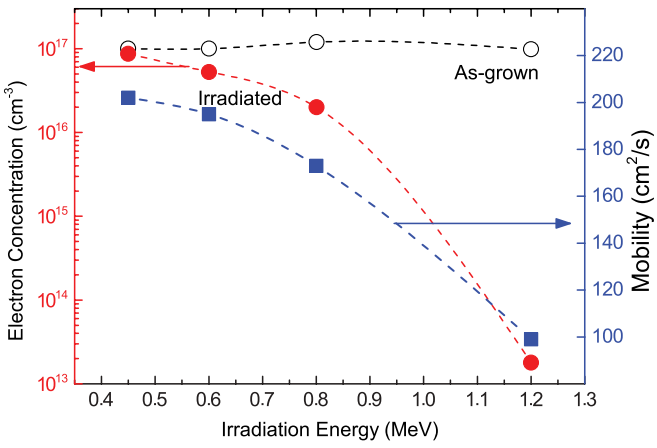

FIG. 1. (Color online) Room temperature Hall carrier concentration and mobility in electron irradiated samples as a function of irradiation energy. The as-grown carrier concentrations were measured on samples taken from the same wafer as the irradiated ones to ensure a valid comparison. The lines are drawn to guide the eye only.

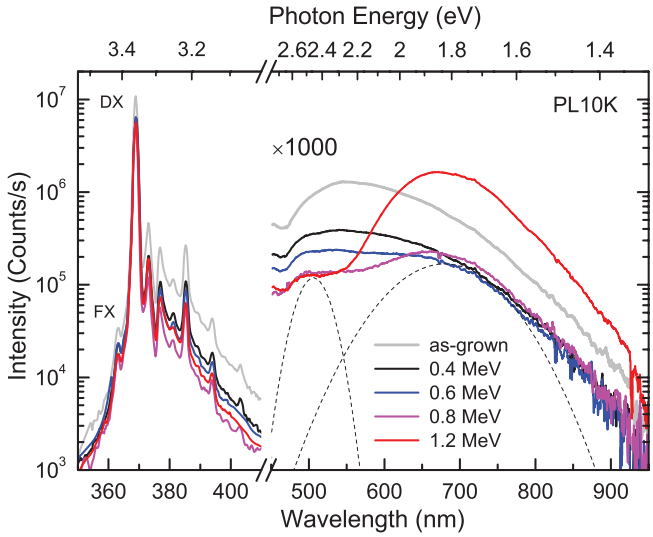

FIG. 2. (Color online) PL spectra from electron irradiated samples measured at 10 K. Note a $\times$1000 prefactor for the deep level related emission components. Dashed lines indicate the position and width of the observed red and green emission bands. *FX* and *DX* denote free and donor-bound exciton recombination, respectively.

directly using the PAS technique. Concentration values below the detection limit are observed in the samples irradiated at 0.45–0.6 MeV τ_{avg} ~170 ps, corresponding to $\lesssim 10^{15}$ cm^{-3} (Refs. 12 and 13). At 0.8 MeV, the average positron lifetime is slightly higher ($\tau_{\mathrm{avg}} \sim$ 171 ps), indicating a zinc vacancy concentration $[V_{\mathrm{Zn}}]$ close to the detection limit. For the 1.2 MeV case, $[V_{\mathrm{Zn}}] = 6 \times 10^{15}$ cm^{-3} and, assuming double ionization, this corresponds to a compensating hole concentration of ~1.2×10^{16} cm^{-3}, which is too low to account for the observed decrease in carrier concentration. The V_{Zn} introduced at low fluences are isolated vacancies according to a study by Zubiaga *et al.*[15] Moreover, an ionic acceptor was observed to dominate the positron trapping at temperatures below 90 K in the 1.2 MeV irradiated sample, resulting in an average lifetime returning to the bulk value (~170 ps). This is in agreement with previous irradiation studies using 2 MeV electrons[13,14] and indicates the presence of negatively charged interstitial or substitutional acceptors.

To shed more light on the balance of intrinsic defects, photoluminescence measurements were performed. Figure 2 shows low temperature PL spectra as a function of electron irradiation energy. A monotonous decrease of the near band edge emission (NBE) intensity occurs with an increase of electron energy. However, the most prominent changes take place in the spectral region related to the deep level emission (DLE), on which we will focus in what follows. Here, two broad emission components can be distinguished at ~510 nm (~2.45 eV) and ~680 nm (~1.75 eV), hereafter referred to as *green* and *red* emission, respectively. These DLE components exhibit notably dissimilar behavior upon electron irradiation. While the green emission is gradually quenched with increasing electron energy, the red emission shows the opposite trend, reaching the highest intensity after 1.2 MeV irradiation. Temperature dependencies of the red and green emission bands are also notably different, as evidenced by the Arrhenius plot in Fig. 3. In contrast to modest developments

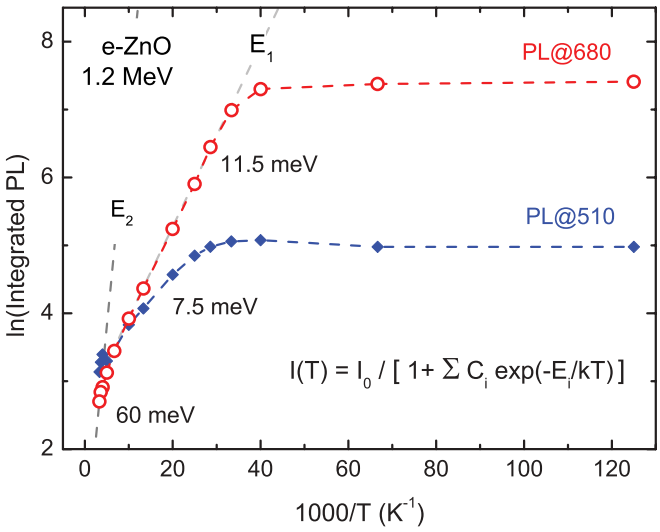

FIG. 3. (Color online) Temperature dependencies of the integrated PL intensity at red (PL@680 nm) and green (PL@510 nm) emission bands in a 1.2 MeV irradiated sample.

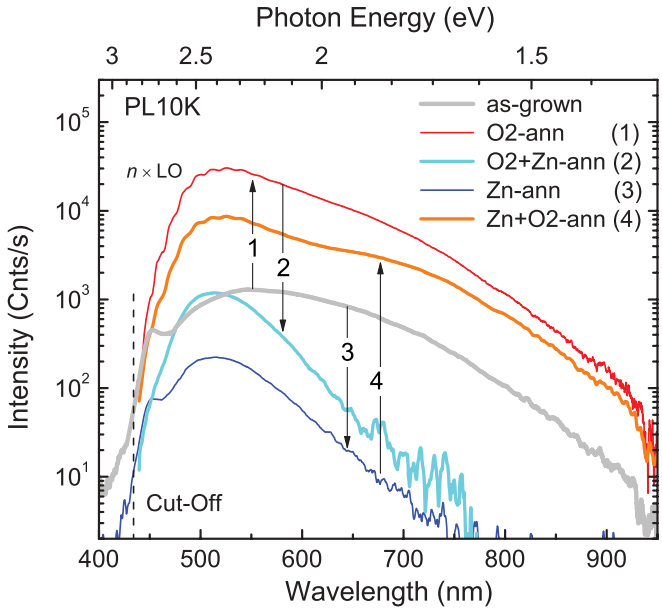

FIG. 4. (Color online) Evolution of deep level related PL spectra upon thermal treatment in different ambients. The gray curve represents as-grown material, and the numbered arrows indicate subsequent spectral developments caused by (1) annealing in O_2, (2) cross annealing in Zn vapor, (3) annealing in Zn vapor, and (4) cross annealing in O_2. $n \times$ LO denotes the onset of multiple LO phonon replicas.

of the green emission intensity, the red component becomes rapidly quenched starting from relatively low temperatures of ~30 K and exhibits a single activation energy of $E_a =$ 11.5 meV throughout most of the temperature range. The latter points toward a possible involvement of thermal delocalization of excitons bound to shallow donors taking part in radiative transitions with deep V_{Zn} acceptor centers. The energy position of such shallow states then could be approximated from the estimated localization energy by applying Haynes rule with the coefficients typically referred to in literature,[16] i.e., $E_{loc} = 0.365 \times E_D - 3.8$ meV. The estimated donor energy $E_D \sim 41.9$ meV is close to that reported for hydrogen related recombination [$E_D = 46.1$ meV (Ref. 16)] and zinc interstitial related shallow donors [$E_D = 37$ meV (Ref. 17)]. It should be noted at this point that there might be other reasons for the red band quenching with a small activation energy. In particular, assume a temperature-dependent capture cross section of the carriers at point defects, or rather their complexes, which are commonly believed to act as nonradiative recombination centers in ZnO. Although thermal activation of a dominant nonradiative channel could lead to similar quenching trends,[18] such a model nonetheless fails to explain why green and red bands are quenched with different activation energies.

In general, the samples annealed in oxygen ambient showed increased resistivity, whereas zinc vapor annealing caused the resistivity to drop. Figure 4 summarizes the effects of sequential postgrowth treatment for the DLE. Considering the as-grown sample as a reference, annealing in oxygen ambient leads to an increase of the DLE intensity by more than one order of magnitude, in contrast to an only somewhat decreased NBE intensity (not shown). On the other hand, Zn ambient annealing causes both an overall decrease in the luminescence intensity and a considerably suppressed red emission band. Subsequent cross annealing demonstrates in both cases a close to full recovery from the effects first introduced by the initial anneal in oxygen or zinc ambient. This suggests that the origin of the two emission components is neither related to extended defects, nor to residual impurities only, but involves point defects, the balance of which is determined by the chemical equilibrium.

Figure 5 summarizes the observed electron irradiation and annealing effects. It should be emphasized that no annealing was performed on the irradiated samples. As discussed above,

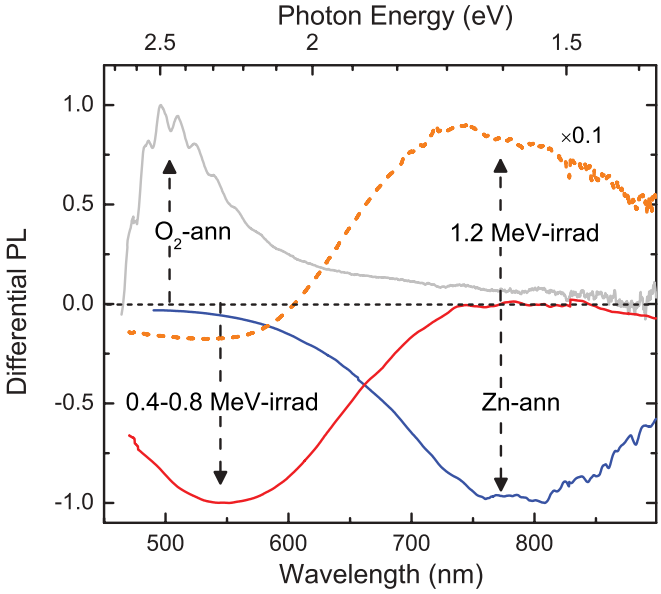

FIG. 5. (Color online) Differential PL spectra, summarizing annealing and electron irradiation effects with respect to as-grown material. The magnitude of spectral changes is normalized for each curve while maintaining the sign.

the defect generation in the low electron irradiation energy range corresponding with a reduction in intensity of the green emission is most likely due to damage on the oxygen sublattice. By the same argument, the red emission band, which is most prominent upon 1.2 MeV irradiation and also weakly present at 800 keV, but not at lower energies, is most likely related to damage on the zinc sublattice. The prime candidates of point defects involved are V_O and O_i on the oxygen sublattice, and V_{Zn} and Zn_i on the zinc sublattice. The latter, Zn_i, is a shallow donor and may participate in DLE primarily via a donor-to-acceptor pair recombination process.[19] Moreover, for the sample annealed in Zn ambient, the red emission is reduced (Fig. 5), strongly suggesting that it is related to the V_{Zn}. Indeed, as indicated by PAS measurements, no V_{Zn} ($\lesssim 10^{15}$ cm^{-3}) could be seen after irradiating samples with energies below 0.8 MeV. At 0.8 MeV, the slight increase in positron lifetime indicates a V_{Zn} concentration close to the detection limit, while for the 1.2 MeV sample it is estimated to be 6×10^{15} cm^{-3}. These PAS results correlate well with the PL data, showing that the intensity of the red emission is increased after the 0.8 and 1.2 MeV irradiations, and also reduced after the Zn-ambient annealing as corroborated by Zubiaga *et al.*[20] The ratio between the red PL intensity[21] of samples irradiated at 1.2 and 0.8 MeV is $I_{1.2}/I_{0.8} \approx 6$, and $[V_{Zn}] = 6 \times 10^{15}$ cm^{-3} in the 1.2 MeV sample. Based on this, we estimate that $[V_{Zn}] \approx 1 \times 10^{15}$ cm^{-3} in the 0.8 MeV sample, consistent with the slight increase observed for the positron lifetime (brackets denote concentration values). These findings enable an unambiguous association of the red DLE component to the zinc vacancy, as also corroborated by Dong *et al.*[8] using depth-resolved cathodoluminescence measurements in combination with PAS.

Regarding the green emission, the intensity increases upon annealing in oxygen ambient, and decreases strongly after electron irradiation, irrespective of energy. The former may suggest that O_i causes this emission, as the concentration of O_i is expected to increase during the oxygen ambient anneal. However, the latter result implies that the green emission, albeit related to oxygen sublattice damage, is not linked to isolated V_O or O_i, since both of these are anticipated to increase in concentration upon irradiation. Instead, this leads us to consider nonradiative complexes as an explanation for the observed behavior. Indeed, the green emission is commonly associated with residual copper impurities,[7,22–24] and Cu is typically present with a concentration of $\sim 10^{15}$ cm^{-3} in Cermet material.[25] If such a copper related emission is partially quenched by V_O present in as-grown material, subsequent annealing in the oxygen ambient activates Cu, which acts both as a compensating and radiative acceptor. Electron irradiation, on the other hand, would generate an excess of V_O, which in turn may further quench the emission by forming nonradiative Cu_{Zn}-V_O complexes. However, also a similar excess of O_i is generated during the irradiation and one may ask why O_i is not filling the open volume in the Cu_{Zn}-V_O complex with the same rate as the formation. A possible explanation may be that the complex is neutral, and competing reactions with active donors prevail for O_i. Moreover, recent experiments show that H implantation passivates the green emission,[26] further strengthening the argument that an acceptorlike defect is involved. In addition, the fine structures on the high energy slope of the green emission in the samples annealed in the oxygen ambient is related to longitudinal optical (LO) phonon replicas with an energy spacing of ~72 meV, implying strong electron-phonon coupling with the estimated Huang-Rhys factor of $S \sim 5.5$. In Ref. 22 very similar phonon modes were observed in Cermet material and identified as Cu_{Zn} impurities, supporting the argument above. Here, it can be pointed out that this argument also holds for other zinc sublattice acceptor impurities, such as Au and Ag.

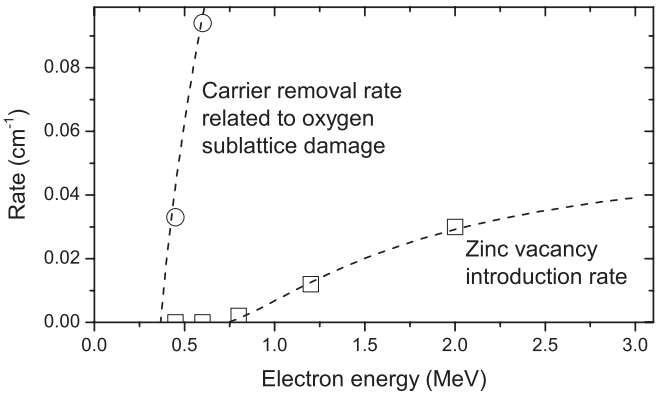

FIG. 6. Squares indicate estimated zinc vacancy introduction rate as a function of electron irradiation energy based on PAS measurements (2 MeV data point from Ref. 13). Circles indicate the carrier removal rate as a function of electron irradiation energy based on Hall effect measurements. Dashed lines are included to guide the eye only.

As unveiled in Fig. 6, the generation rate of V_{Zn} is insufficient to account for the observed loss of charge carriers. In particular, the loss is especially pronounced at electron energies below the threshold for generation of zinc sublattice defects. A more suitable candidate is O_i, which can exist in a doubly negative (or neutral) charge state in n-type material.[19] In fact, the presence of oxygen interstitials, or a compensating acceptor complex involving O_i, is fully corroborated by the ionic acceptor observed by PAS and the low electron mobility as a result of ionized impurity scattering observed by Hall measurements.

The introduction rate of V_{Zn} is low compared with that of compensating oxygen sublattice defects, implying a high degree of self-annihilation on the zinc sublattice, which is in accordance with previous observations of a strong radiation hardness of ZnO.[13] Applying the McKinley-Feshbach model,[27] the displacement energies for the Zn and O atoms are estimated to be 43 and 68 eV, respectively. These values compare reasonably well with those reported previously in the literature,[10,28,29] and in particular, the displacement energy of O is much higher than that of Zn.

Conclusion. After subjecting ZnO samples to sequential annealing in oxygen and zinc atmospheres (and vice versa) as well as to variable energy electron irradiation, we extract complementary information from PAS and PL measurements which is used to identify V_{Zn}. The characteristic red PL band at ~1.75 eV is unambiguously associated with an optical transition involving V_{Zn}-related deep acceptors and residual shallow donors, possibly including Zn_i which is likely present in high concentrations in MeV electron irradiated samples. It is found that at electron energies $\gtrsim$0.8 MeV, damage is inflicted

upon the zinc sublattice resulting in $[V_{Zn}] = 6 \times 10^{15}\,cm^{-3}$ for a fluence of 5×10^{17} cm^{-2} at 1.2 MeV. The loss of charge carriers upon electron irradiation is predominantly due to defects on the oxygen sublattice and strong evidence is obtained that O_i is the dominating acceptor. Evidence is also presented indicating that the green PL emission is caused by acceptor impurities which may be passivated by V_O introduced via irradiation or reducing atmosphere.

Acknowledgments. Financial support from the Research Council of Norway, provided through the FRINAT project Understanding ZnO, as well as from NordForsk/LENS collaboration is acknowledged.

[1] A. Janotti and C. G. Van de Walle, Rep. Prog. Phys. **72**, 126501 (2009).
[2] C. G. Van de Walle, Physica B: Condens. Matter **308–310**, 899 (2001).
[3] E. C. Lee, Y. S. Kim, Y. G. Jin, and K. J. Chang, Phys. Rev. B **64**, 085120 (2001).
[4] T. M. Børseth, B. G. Svensson, A. Yu. Kuznetsov, P. Klason, Q. Zhao, and M. Willander, Appl. Phys. Lett. **89**, 262112 (2006).
[5] K. Vanheusden, C. H. Seager, W. L. Warren, D. R. Tallant, and J. A. Voigt, Appl. Phys. Lett. **68**, 403 (1996).
[6] B. Lin, Z. Fu, and Y. Jia, Appl. Phys. Lett. **79**, 943 (2001).
[7] R. Dingle, Phys. Rev. Lett. **23**, 579 (1969).
[8] Y. Dong, F. Tuomisto, B. G. Svensson, A. Yu. Kuznetsov, and L. J. Brillson, Phys. Rev. B **81**, 081201 (2010).
[9] W. E. Vehse, W. A. Sibley, F. J. Keller, and Y. Chen, Phys. Rev. **167**, 828 (1968).
[10] J. M. Meese and D. R. Locker, Solid State Commun. **11**, 1547 (1972).
[11] D. R. Locker and J. M. Meese, IEEE Trans. Nucl. Sci. **19**, 237 (1972).
[12] K. Saarinen, P. Hautojarvi, and C. Corbel, in *Identification of Defects in Semiconductors, Vol. 51A* of *Semiconductors and Semimetals*, edited by M. Stavola (Elsevier, Amsterdam, 1998), pp. 209–285.
[13] F. Tuomisto, V. Ranki, K. Saarinen, and D. C. Look, Phys. Rev. Lett. **91**, 205502 (2003).
[14] F. Tuomisto, K. Saarinen, D. C. Look, and G. C. Farlow, Phys. Rev. B **72**, 085206 (2005).
[15] A. Zubiaga, F. Tuomisto, V. A. Coleman, H. H. Tan, C. Jagadish, K. Koike, S. Sasa, M. Inoue, and M. Yano, Phys. Rev. B **78**, 035125 (2008).
[16] B. K. Meyer, H. Alves, D. M. Hofmann, W. Kriegseis, D. Forster, F. Bertram, J. Christen, A. Hoffmann, M. Strassburg, M. Dworzak, U. Haboeck, and A. V. Rodina, Phys. Status Solidi B **241**, 231 (2004).
[17] J. Sann, J. Stehr, A. Hofstaetter, D. M. Hofmann, A. Neumann, M. Lerch, U. Haboeck, A. Hoffmann, and C. Thomsen, Phys. Rev. B **76**, 195203 (2007).
[18] J. Krustok, H. Collan, and K. Hjelt, J. Appl. Phys. **81**, 1442 (1997).
[19] A. Janotti and C. G. Van de Walle, Phys. Rev. B **76**, 165202 (2007).
[20] A. Zubiaga, F. Plazaola, J. A. Garcia, F. Tuomisto, V. Munoz-Sanjose, and R. Tena-Zaera, Phys. Rev. B **76**, 085202 (2007).
[21] Intensity-dependent measurements were performed (not shown) to ensure linearity between excitation and emission intensity.
[22] M. A. Reshchikov, H. Morkoç, B. Nemeth, J. Nause, J. Xie, B. Hertog, and A. Osinsky, Physica B: Condens. Matter **401-402**, 358 (2007).
[23] N. Y. Garces, L. Wang, L. Bai, N. C. Giles, L. E. Halliburton, and G. Cantwell, Appl. Phys. Lett. **81**, 622 (2002).
[24] D. Byrne, F. Herklotz, M. Henry, and E. McGlynn, J. Phys.: Condens. Matter **24**, 215802 (2012).
[25] M. D. McCluskey and S. J. Jokela, Physica B: Condens. Matter **401**, 355 (2007).
[26] See Supplemental Material at http://link.aps.org/supplemental/10.1103/PhysRevB.86.121203 for a copy of an unpublished paper by Z. Zhang, D. C. Look, K. M. Johansen, B. G. Svensson, and L. J. Brillson. This paper describes H-implanted hydrothermal ZnO, in which the 2.5 eV emission, as measured by cathodoluminescence, is quenched by the introduction of H.
[27] F. Agulló-López, C. R. A. Catlow, and P. D. Townsend, *Point Defects in Materials* (Academic, London, 1988).
[28] D. C. Look, G. C. Farlow, P. Reunchan, S. Limpijumnong, S. B. Zhang, and K. Nordlund, Phys. Rev. Lett. **95**, 225502 (2005).
[29] R. E. Williford, R. Devanathan, and W. J. Weber, Nucl. Instrum. Methods Phys. Res., Sect. B **141**, 94 (1998).